Accepted Manuscript

Title: The proteome of *Medicago truncatula* in response to ammonium and urea nutrition reveals the role of membrane proteins and enzymes of root lignification

Authors: Beatriz Royo, Raquel Esteban, Javier Buezo, Enrique Santamaría, Joaquín Fernández-Irigoyen, Dirk Becker, Jose F. Moran

PII: S0098-8472(18)31562-4
DOI: https://doi.org/10.1016/j.envexpbot.2019.02.010
Reference: EEB 3698

To appear in: *Environmental and Experimental Botany*

Received date: 12 October 2018
Revised date: 6 February 2019
Accepted date: 6 February 2019

Please cite this article as: Royo B, Esteban R, Buezo J, Santamaría E, Fernández-Irigoyen J, Becker D, Moran JF, The proteome of *Medicago truncatula* in response to ammonium and urea nutrition reveals the role of membrane proteins and enzymes of root lignification, *Environmental and Experimental Botany* (2019), https://doi.org/10.1016/j.envexpbot.2019.02.010

The proteome of *Medicago truncatula* in response to ammonium and urea nutrition reveals the role of membrane proteins and enzymes of root lignification

Beatriz Royo[a], Raquel Esteban[b], Javier Buezo[a], Enrique Santamaría[c], Joaquín Fernández-Irigoyen[c], Dirk Becker[d], Jose F. Moran[a*]

[a]*Department of Science, Institute of Multidisciplinary Applied Biology (IMAB), Public University of Navarre (UPNA), Avenida de Pamplona 123, 31192 Mutilva, Spain*
[b]*Department of Plant Biology and Ecology, University of the Basque Country (UPV/EHU), c/ Sarriena s/n; apdo. 644, Bilbao, Spain*
[c]*Proteomics Unit, Navarrabiomed, Fundación Miguel Servet, Proteored-ISCIII, Navarra Institute for Health Research (IdISNA), Pamplona, Spain*
[d]*Plant Molecular Biology & Biophysics, University of Würzburg, 97082 Würzburg, Germany*

Corresponding author:
Dr. Jose F. Moran
Tel: +34 948168018
jose.moran@unavarra.es

Other email addresses:
Beatriz Royo: beatriz.royo@unavarra.es
Raquel Esteban: raquel.esteban@ehu.es
Javier Buezo: javier.buezo@unavarra.es
Enrique Santamaría: enrique.santamaria.martinez@navarra.es
Joaquín Fernandez-Irigoyen: jfernani@navarra.es
Dirk Becker: dirk.becker@uni-wuerzburg.de

Highlights

- The root proteome of *M. truncatula* as a response to the N source is dissected.
- Differentially accumulated membrane proteins regulate the intracellular pH.

- Phenylpropanoids metabolism affects the stunted roots of ammonium-grown plants.
- The modulation of peroxidases contributes to the reinforcement of cell wall.
- The higher lignification of root cells contributes to the ammonium tolerance.

Abstract

Plants differ widely in their growth and tolerance responses to ammonium and urea nutrition, while derived phenotypes seem markedly different from plants grown under nitrate supply. Plant responses to N sources are complex, and the traits involved remain unknown. This work reports a comprehensive and quantitative root proteomic study on the NH_4^+-tolerant legume *Medicago truncatula* grown under axenic conditions with either nitrate, NH_4^+ or urea supply as sole N source by using the iTRAQ method. Sixty-one different proteins among the three N sources were identified. Interestingly, among the proteomic responses, urea nutrition displayed greater similarity to nitrate than to ammonium nutrition. We found remarkable differences in membrane proteins that play roles in sensing the N form, and regulate the intracellular pH and the uptake of N. Also, several groups of proteins were differentially expressed in the C metabolism pathway involved in reorganizing N assimilation. In addition, enzymes related to phenylpropanoid metabolism, including the peroxidases POD2, POD6, POD7 and POD11, which were up-regulated under ammonium nutrition, contributed to the reinforcement of cell walls, as confirmed by specific staining of lignin. Thus, we identified cell wall lignification as an important tolerance mechanism of root cells associated with the stunted phenotype typical of plants grown under ammonium nutrition

Abbreviations: abscisic acid (ABA); ammonia (NH_3); ferulic acid (FA); ferulic acid peroxidase (FPX); Gen Ontology Annotation (GOA); guiacol peroxidase (GPX); Guaiacyl lignin (G); jasmonate (JA); Kyoto Encyclopedia of Genes and Genomes (KEGG); lipoxygenase (LOX); mass spectrometry (MS); nitrogen (N); phenylpropanoids (PP); peroxidase activity (POD); Syringyl lignin (S).

Keywords: Ammonium, lignin, *Medicago truncatula*, peroxidase, phenylpropanoid, urea.

1. Introduction

In natural soils, nitrogen availability is compromised by several environmental factors (e.g. pH, organic matter, temperature etc.) that affect plant growth and limit the productivity of agricultural ecosystems (Li et al., 2001). The current world demand for food production requires the intensive utilization of fertilizers and manures, in the form of nitrate, ammonium and/or urea, with a high environmental cost including global climate change and biodiversity loss. Plants can take up and use nitrogen (N) as nitrate, ammonium or urea. The nature of the N source determines diverse signalling pathways and thus, differentially affects plant development and cell metabolism. Indeed, ammonium is taken up preferentially at low concentrations, but above a certain threshold it becomes toxic to most plants (Britto and Kronzucker, 2002; Esteban et al., 2016a). This toxicity depends on ammonium concentration and plant species or variety tolerance (Cruz et al., 2011; Gerendas et al., 1997; Li et al., 2014). Similar to ammonium, toxic effects on plants have also been reported for urea, but with a lower degree of severity (Houdusse et al., 2005). *Medicago truncatula* Gaertn. is able to grow exclusively with ammonium or urea as the sole N source, even at high doses (25 mM) (Esteban et al., 2016b). Thus, in comparison to many other plant species, *M. truncatula* is characterized as tolerant of ammonium nutrition. However, the plant traits responsible for ammonium and/or urea tolerance remain unknown and so understanding this tolerance and the molecules implicated in differential nitrogen nutrition is an environmental priority.

Roots constitute the first nutrient sensor, and to guarantee adequate N acquisition the roots adapt their phenotype and physiology to differential N nutrition (Esteban et al., 2016b; Forde, 2014; Nacry et al., 2013). Accordingly, stunted root growth is among the most visible phenotypic responses to ammonium nutrition in *Arabidopsis* (Britto and Kronzucker, 2002; Li et al., 2014; Liu et al., 2013). With respect to nitrate supply, the *M. truncatula* phenotype under ammonium and urea nutrition is characterized by changes in the main root elongation rate, the number and length of lateral roots, and the positioning of lateral roots relative to the root tip (Esteban et al., 2016b). Several molecular mechanisms underlying various aspects of ammonium sensitivity in plants have been identified. These include GDP-mannose pyrophosphorylase activity for the inhibition of root elongation (Qin et al., 2008), potassium transporters for the loss of root gravitropism (Zou et al., 2012) and ethylene receptor signalling for the inhibition of

lateral root formation (Li et al., 2013). In contrast, molecular determinants of urea sensitivity are largely unknown.

Using iTRAQ quantitative mass spectrometry (MS) proteomics, this study aimed to identify proteins and traits involved in the tolerance response to ammonium and urea nutrition in *Medicago truncatula* in contrast to the acute toxicity-response that can be observed in sensitive plants like *Arabidopsis* (Marino et al., 2016). We have found a significant involvement of membrane proteins and a role for phenylpropanoids (PP) as determinants of ammonium tolerance. The relevance of our findings for the mechanisms underlying ammonium and urea tolerance is discussed.

2. Materials and methods

2.1. Plant growth conditions and length measurement

Medicago truncatula ecotype Jemalong A17 seeds were scarified, sterilized, germinated and grown as explained in Esteban et al. (2016b). The nutrient medium contained 1mM N applied as $Ca(NO_3)_2$, $(NH_4)_2SO_4$ or urea. This concentration was selected so that we could focus more on the proteome differences among the different N treatments than the stress caused by high N conditions. In order to isolate the plant response from possible interacting microorganisms, plants were grown under axenic conditions. During the preparation of the axenic media, the pH was carefully controlled before and after autoclaving to ensure a specific pH of 6.5 at the time that the seeds were sown. Briefly, Ca and N forms were sterilized by filtration. All the other nutrients were mixed, pH adjusted to 6.5, agar supplemented, and then autoclaved. At a later stage, Ca and N were added to the autoclaved media before solidification, and an aliquot of each was taken to measure the pH again. In order to compensate for the Ca^{+2} supplied with the NO_3^- treatment, the ammonium- and urea-fed plants were supplemented with 0.5 mM $CaSO_4$. The plants were grown in a growth chamber for 15 days at a day/night temperature of 24.5/22 ºC, under 80 % relative humidity, with a 16/8 h day/night photoperiod and 70 µmoles m^{-2} s^{-1} of photosynthetically active radiation. During the harvest, a pool of roots from five plants from different pots was collected for every replicate, and this was weighed, frozen in liquid N_2 and stored at -80 ºC for further analyses. Plants were carefully harvested from their pots, placed on absorbent paper and then plant root length was measured with a ruler.

2.2. Total protein extraction and sample labelling for iTRAQ analysis

The total proteins of *M. truncatula* roots were extracted from 300 mg of frozen tissues. Roots were ground in liquid N_2 using a mortar and pestle with the addition of a protease inhibitor. Powdered samples were homogenized with 500 µl of extraction buffer (7 M urea, 2 M thiourea, 4% (w/v) CHAPS, 2% (v/v) Triton X-100 and 50 mM DTT) to maximize the extraction of water-soluble and membrane proteins. The homogenate was centrifuged at 10000*g* and 4 ºC for 10 min. Supernatants containing the root proteins (150 µg) were precipitated with methanol/chloroform, and then the obtained pellets were suspended in a mixture of 7 M urea, 2 M thiourea and 4% (v/v) CHAPS. The protein content of every extract (three biological replicates for nitrate and ammonium nutrition, and two for urea) was quantified with a Bradford assay kit (Bio-Rad) prior to carrying out the comparative proteomic analysis of proteins using the isobaric Tags for Relative and Absolute Quantitation (iTRAQ) approach (Unwin et al., 2010). The samples were iTRAQ-labelled according to the manufacturer's protocol (Sciex) as follows: 100 µg of protein from each sample were reduced with 50 mM tris (2-carboxyethyl) phosphine (TCEP) at 60 °C for 1 h. Then, cysteine residues were alkylated with 200 mM methylmethanethiosulfonate (MMTS) at room temperature for 15 min. Trypsin (Promega; 1:20, w/v) was used to cleave the protein mix for 16 h at 37 ºC, and every tryptic digest was labelled with an isobaric amine-reactive tag by incubation for 1 h (iTRAQ 8-plex experiment). Finally, every set of labelled samples was independently pooled and evaporated in a vacuum centrifuge until a volume lower than 40 µl was reached.

2.3. Peptide fractionation by HPLC and mass spectrometry analysis

In order to increase proteome coverage, peptide fractionation was performed before characterization of the proteins. The peptide pool was injected into an Ettan LC system with an X-Terra RP18 pre-column (2.1 x 20mm) and a high pH stable X-Terra RP18 column (C18; 2.1mm x 150mm; 3.5µm) (Waters) at a flow rate of 40 µl/min. Peptides were eluted using a mobile phase B linear gradient of 5–65% over 35 min (A, 5 mM ammonium bicarbonate in water at pH 9.8; B, 5 mM ammonium bicarbonate in acetonitrile at pH 9.8). Then, 11 fractions were collected, evaporated under vacuum and

reconstituted into 20 µl of 2% acetonitrile, 0.1% formic acid, and 98% milli-Q H_2O prior to MS analysis.

The peptide mixtures contained in each fraction were separated by reverse-phase chromatography using an Eksigent nanoLC ultra 2D pump fitted with a 75 µm ID column (Eksigent 0.075 x 25cm). Initially, samples were loaded for desalting and concentration into a 0.5 cm length and 300 µm ID pre-column packed with the same chemistry as the separating column. Mobile phases were 0.1% formic acid in 100% water as buffer A and 0.1% formic acid in 100% acetonitrile as buffer B. The column gradient was developed as a two-step gradient from 5% B to 25% B in 180 min and 25% B to 40% B in 30 min. The column was equilibrated in 95% B for 10 min and 5% B for 15 min. During the processes, the pre-column was in line with the column and flow was maintained along the gradient at 300 nl/min. Eluting peptides from the column were analysed using a Sciex 5600 TripleTOF™ system. Data were acquired from a survey scan performed in a mass range from 350 m/z up to 1250 m/z in a scan time of 250 ms. The top 35 peaks were selected for fragmentation. Minimum accumulation time for MS/MS was set to 100 ms giving a total cycle time of 3.8 s. Product ions were scanned in a mass range from 100 m/z up to 1700 m/z and excluded for further fragmentation over 15 s.

2.4. Proteomic data analysis

The raw data (wiff, Sciex) were analysed with *MaxQuant* software (Cox and Mann, 2008). For peak list generation, default Sciex Q-TOF instrument parameters were used except for the main search peptide tolerance and MS/MS match tolerance, which were set to 0.01 Da and increased up to 50 ppm, respectively. A contaminant database (.fasta) was used for filtering out contaminants. Peak lists were searched against a JCVI database (http://www.jcvi.org/medicago) of *Medicago truncatula* protein sequences, and Andromeda was used as a search engine (Cox et al., 2011). Methionine oxidation was set as the variable modification, and the carbamidomethylation of cysteine residues was set as the fixed modification. Reporter ion intensities were bias corrected for the overlapping isotope contributions from the iTRAQ tags according to the certificate of analysis provided by the reagent manufacturer (Sciex). The peptide and protein selection criteria for relative quantitation were performed as follows. Maximum false

discovery rates (FDR) were set to 0.01 at protein and peptide levels. Analyses were limited to peptides of six or more amino acids in length, and considering a maximum of two missed cleavages. The output data files with the relative protein abundance were managed using R scripts for subsequent statistical analyses and representation. Proteins identified by site (identification based only on a modification), reverse proteins (identified by a decoy database) and potential contaminants were filtered out. Only proteins with more than one identified peptide were used for quantification. For the possible rescue of quantification data, up to one missing value for each group was rescued, replacing it by the mean of the rest of the in-group samples. Data were normalized and transformed for later comparison using quantile normalization and log2 transformation, respectively. The Limma Bioconductor software package in R was used for ANOVA analyses. Significant and differential data were selected by a *p*-value lower than 0.01, fold changes of <0.77 (down-accumulation) and >1.3 (up-accumulation) in linear scale. MS raw data and search results files have been deposited in the ProteomeXchange Consortium (http://proteomecentral.proteomexchange.org) via the PRIDE partner repository (Vizcaíno et al., 2016) with the dataset identifiers PXD011074.

2.5. Protein analysis and classification

Data mining was performed using bioinformatic tools. Hence, the functional classification of the differentially accumulated proteins was realized according to the Gene Ontology Annotation (GOA) consortium and using the QuickGo browser (https://www.ebi.ac.uk/QuickGO/) developed by the European Bioinformatics Institute (EMBL-EBI) (Binns et al., 2009). Proteins were also clustered into orthologous groups using the eggNOG 4.5 database (Huerta-Cepas et al., 2016). Moreover, the identified proteins were studied with the Kyoto Encyclopedia of Genes and Genomes (KEGG) and the enriched metabolic pathways were analysed with the KOBAS 3.0 pathway mapping tool (http://kobas.cbi.pku.edu.cn/). The ClustalW tool was used to perform the multiple sequence analysis of lignin-associated peroxidases and to study their phylogenetic relationships (McWilliam et al., 2013; Sievers et al., 2011).

2.6. Peroxidase activity assay

The peroxidase activity in the presence of guaiacol (guaiacol peroxidase, GPX) and ferulic acid (ferulic acid peroxidase; FPX) as substrates were measured in root extracts. 0.2 g of frozen roots were extracted by homogenization at 4 ºC with 50 mM potassium phosphate pH 6.0, 1 mM EDTA, 2 mM DTT, 0.5% (v/v) TRITON and 1.5% (w/v) PVPP, and subsequent centrifugation at 16000*g* for 20 min. The activities were assayed after the addition of 10 µl of the plant extract to a mixture composed of 50 mM sodium phosphate pH 6.0, 5 mM H_2O_2 and 1 mM of either guaiacol or ferulic acid. The GPX and FPX activities were estimated by following the oxidation of either guaiacol or ferulic acid for 2 minutes at a wavelength of 470 nm (ε=26.6 $mM^{-1}cm^{-1}$) or 310 nm (ε=16.3 mM^{-1} cm^{-1}), respectively (Cordoba-Pedregosa et al., 1996; Stasolla and Yeung, 2007).

2.7. Lignin staining and microscopy

Root fragments of approximately 2 mm were submerged in Safranin-O (0.1%) for 2 minutes and thoroughly washed with water. An Olympus SZ40 transmission light microscope with an Olympus E510 camera was used for image acquisition. The images were analysed with ImageJ software (Schneider et al., 2012) for staining intensity quantification.

2.8. Statistics

Differences among nutrition types were evaluated with one-way ANOVA and post-hoc Student-Newman-Keuls tests. All data were tested for normality (Kolmogorov–Smirnof test) and homogeneity of variances (Levenne test). The resulting *p* values were considered to be statistically significant at $\alpha = 0.05$. Statistical analyses were performed with IBM SPSS Statistics for Windows, Version 21.0. Armonk, NY: IBM Corp

3. Results

3.1. The N source shapes the *Medicago truncatula* proteome root profile

In order to gain insight into the proteomic response of plants subjected to different N nutrition, we analysed the root proteome using iTRAQ-MS. In order to isolate the plant

response from possible interacting microorganisms, plants were grown under axenic conditions. Plants cultured in the presence of ammonium or urea as the sole N source grew without toxicity symptoms (Esteban et al., 2016b). However, the ammonium-fed seedlings exhibited a stunted root phenotype (Fig. 1), a common symptom of ammonium nutrition. Additional data on the Root System Architecture of *M. truncatula* grown under ammonium and urea nutrition are available in a previous work (Esteban et al., 2016b). Following MS analysis and low-scoring spectra filtering, we identified 1533 distinct root proteins of which 1126 were quantified (Supplementary Dataset S1). These quantified proteins were clustered into groups of homologues by aligning all proteins with highly significant alignment scores (Supplementary Fig. S1). The final dendrogram depicted in Supplementary Fig. S1 demonstrated a strong correlation among the replicates within all three nutritional treatments. Furthermore, the dendrogram indicated that the cluster of proteins identified after urea treatment had a greater similarity to the nitrate protein cluster, whereas the ammonium cluster was represented as an out-group. Based on a significance level of $p < 0.01$ and a 1.3-fold change cut-off (Supplementary Fig. S2), 61 differentially regulated proteins were identified in the ammonium and urea clusters with respect to nitrate control conditions (Table 1).

Among those 61 proteins, 53 proteins were differentially accumulated under ammonium nutrition relative to nitrate conditions (Fig. 2). On the other hand, urea-grown roots showed a smaller number of differentially regulated proteins (29; Fig. 2). Moreover, 21 proteins were shared between the responses to ammonium or urea nutrition with respect to nitrate nutrition (Fig. 3). Seven out of these 21 proteins were up-accumulated while 13 of the remaining proteins were down-accumulated. The last of the 21 proteins, ribulose bisphosphate carboxylase/oxygenase (RuBisCo)-activase, was identified as a unique protein differentially regulated between ammonium and urea relative to nitrate nutrition (Fig. 3; Table 1), being up-accumulated under ammonium and down-accumulated under urea.

3.2. Functional classification of the differentially accumulated proteins

According to Gene Ontology (GO) categories, the differentially accumulated proteins were classified on the basis of biological processes, molecular function and cellular component using GO Slim, which is a more specific hit finder than GO (Fig. 4). Most of

the proteins were involved in metabolic, cellular and biosynthetic processes and about 33% were involved in responses to both biotic and abiotic stimuli (Fig. 4). Moreover, based on molecular function properties, the 61 proteins were mainly classified into binding (51%) and catalytic (48%) activity. With respect to their cellular localization, is notable that the majority of differentially accumulated proteins were associated with membranes (Fig. 4).

Meanwhile, these proteins were also classified into 13 different functional categories in accordance with the "euKaryotic Orthologous Group of proteins" (KOG) (Fig. 5A, 5B; Table 1). This classification evidenced that carbohydrate transport and metabolism-related proteins in ammonium-fed roots underwent the greatest changes among all categories (Fig. 5A). A group of 4 proteins associated with post-translational modifications and protein turnover ("O" group) were also enriched. As shown in Table 1, these proteins were a Tau class glutathione S-transferase (Tau GST), a glutathione S-transferase amine-terminal domain protein, a peptidyl-prolyl cis-trans isomerase, and RuBisCo activase. In contrast, we found that proteins that belonged to the amino acid, coenzyme and lipid metabolisms, together with secondary metabolites and cell wall/membrane biosynthesis, were all down-accumulated in the ammonium treated plants (Fig. 5A).

On the other hand, under urea nutrition there were changes in fewer functional protein classes compared to ammonium nutrition, and nearly half of the differentially expressed proteins were grouped into the carbohydrate or energy metabolism categories (Fig. 5B). Groups E, J and M showed a down-accumulation of all their proteins. Besides, only one protein was assigned to signal transduction mechanisms (group T). This protein was a chitinase (Medtr7g115220.1), whose relative abundance increased when plants were grown with either ammonium or urea (Fig. 5A, 5B). Chitinases are involved in developmental aspects of plants, and also play a role under both, biotic and abiotic stress situations, in which chitinases are controlled by jasmonic acid (JA) and abscisic acid (ABA) (Grover, 2012). Interestingly, some of the proteins in the non-function assigned group (group S) are also related to the ABA/JA signalling pathway as provided by KOG (Table 1).

3.3. Ammonium nutrition altered the enzyme patterns of phenylpropanoid metabolism

In order to identify pathways enriched in our set of differentially accumulated proteins, we next determined the role of the 61 proteins in the Kyoto Encyclopedia of Genes and Genomes (KEGG) database. As shown in Supplementary Table S1, using a *p*-value threshold of ≤ 0.01, proteins from the ammonium treatment were mainly implicated in metabolic processes, such as the biosynthesis of secondary metabolites and carbon metabolism, as well as the metabolism of some amino acids. The proteome from urea-grown roots was enriched in just 4 pathways that were related to carbon metabolism in particular.

Because ammonium nutrition mainly involved shifts in enzymes related to the production of structural metabolites, such as phenylpropanoids (including stilbenoids and gingerol) examination of the proteins involved is described below. As shown in Table 2, a batch of 8 proteins was differently accumulated into the phenylpropanoid pathway. Considering it in detail, we found that a group of four peroxidases (PODs) and a caffeic acid O-methyltransferase (COMT) protein were up-accumulated, whereas, caffeoyl-CoA 3-O-methyltransferase (CCOMT), cytochrome P450 family cinnamate 4-hydroxylase (CyP450 C4H), and phenylalanine ammonia-lyase-like protein (PAL) were down-accumulated in ammonium grown roots. The CCOMT and CyP450 C4H activities also belong to the stilbenoid, diarylheptanoid and gingerol biosynthesis pathway, whose end products include phenolic compounds, phenolic glycosides, and curcumins from the ginger family. The involvement of these eight differentially identified proteins in phenylpropanoid biosynthesis is depicted in detail in Figure 6. For further assessment, we performed a complementary study for the specific localization of these eight proteins using several prediction servers (see Supplementary Table S2) to ascertain the subcellular pathways that the proteins may follow. Based on the presence or absence of signal peptides in their sequences, five proteins (CyP450 C4H and the four PODs) were inferred as being secreted outside the cell, whereas the other three proteins may be located in the cytoplasm or in the chloroplast.

On the other hand, amino acid biosynthesis was a remarkably enriched pathway that included 4 proteins from the 53 differential proteins identified when growing plants

under ammonium nutrition (Supplementary Table S1). All four of them were down-accumulated (Table 1; Fig. 3), and three of these proteins cobalamin-independent methionine synthase, O-acetylserine (thiol) lyase and S-adenosylmethionine synthase-like protein, also belong to cysteine and methionine metabolism (mtr00270).

We have analysed the amino acid composition of the protein sequences. It has been reported that ammonium stress induces increased synthesis of amino acids with a low ratio C/N, such as asparagine or arginine, and this is related to lower C and high N availability (Ariz et al., 2013). Based on the asparagine content (Hoepflinger et al., 2011), no N enriched proteins were detected among any of the 61 proteins whose accumulation was differentially affected by the source of N. In addition, we later included arginine and histidine in the analysis, but neither of these indicated significant changes (data not shown).

3.4. Ammonium nutrition increased the POD-dependent lignification of cell walls

Analysis of the differential proteome showed that POD proteins were up-accumulated under ammonium treatment, thus implicating POD activity in tolerance to ammonium nutrition in *M. truncatula* plants. In order to confirm the data obtained by iTRAQ analysis, the GPX and the FPX activities were determined in root tissues (Fig. 7). The data we obtained matched with the proteomics results displayed previously (Fig. 3; Fig. 6; Table 1). In particular, GPX was significantly higher in ammonium-fed roots, whereas no significant differences were found between nitrate- and urea-grown roots (Fig. 7A). Moreover, FPX activity was lower in ammonium roots (Fig. 7B), which correlates with the higher accumulation of COMT protein in this treatment compared to urea and nitrate.

Because POD contributes to the synthesis of monolignols, which ultimately form an impermeable layer of lignin between the cell walls of adjacent cells (Lee et al., 2013), the lignification of the studied root cells was analysed by specific staining of lignin with Safranin O (Fig. 8). Roots from the ammonium and urea treatments (although the latter was less intense) presented darker colour intensity than those from nitrate-fed roots, which was observed directly on the light microscope (Fig. 8A). Quantification of the

image colour confirmed this observation, showing that lignification of root cells was significantly higher in the ammonium-treated roots (Fig. 8B).

4. Discussion

4.1. The urea and nitrate proteomes had more similarities than the urea and ammonium proteomes

The analyses revealed that roots expressed a distinct proteome depending on the nutrition on which the seedlings had been grown. Thus, although urea nutrition in plants has been described as producing toxic effects similar to ammonium (Arkoun et al., 2012; Houdusse et al., 2005), in our study, when we clustered the effects of the different forms of N nutrition, there was greater similarity between the altered proteomes of nitrate- and urea-grown roots than between ammonium- and nitrate-grown roots (Supplementary Fig. S1). Urea-fed roots produced a lower number of differentially expressed proteins compared to nitrate-fed roots (Fig. 2, Fig. 3). The N dose used in this work (1 mM) was not enough to observe important differences in the responses between nitrate and urea due to urea being a source of N that plants can use without toxicity (unlike ammonium). Therefore, urea-fed roots maintained optimal growth, and no developmental differences with respect to the nitrate treatment were found (Fig. 1). Altogether, these findings were in agreement with results reported by Esteban et al. (2016b), where plants of *M. truncatula* exhibited no toxic effects when urea was supplied as the only N source. In contrast, ammonium-fed plants exhibited stunted root growth (Fig. 1) and a significantly different proteome from urea and nitrate-based nutrition (Fig. 2, Fig. 3).

Ammonium nutrition has been previously shown to induce a stress that affects the energy and carbon requirements of plants (Ariz et al., 2010). In the current work ammonium, and also urea nutrition, significantly modified some proteins of carbohydrate transport and metabolism, as indicated by the KOG and GO Slim classifications (Table 1, Fig. 4, Fig. 5). The *Enrichment pathway* analysis (Supplementary Table S1) also supported this observation, which suggests that the changes in these proteins may explain the optimal adaptation of the plants when urea is supplied as the only source of N, because urea did not represent a stressful condition

(Fig.1) (Esteban et al., 2016b). In contrast, the ammonium-fed plants needed a complementary metabolism adaptation including the modulation of phenylpropanoid metabolism (Supplementary Table S1), which finally leads to reinforcement of the cell wall (Figs. 6-8). This adaptation may serve as a tolerance response because the performance of the *Medicago truncatula* plants under ammonium in our experimental conditions was substantially affected (Esteban et al., 2016b). This type of adaptation involving proteins of metabolism is in agreement with the results obtained in several proteomic studies of *A. thaliana* when comparing ammonium- vs. nitrate-fed plants (Engelsberger and Schulze, 2012; Marino et al., 2016; Menz et al., 2016). However, as *Arabidopsis* is a highly sensitive species to ammonium, the specific metabolic changes linked with the adaptation to such nutrition were different and an enhancement of glucosinolate metabolism was detected instead of the phenylpropanoid pathway.

Interestingly, *M. truncatula* roots differentially accumulated RuBisCO proteins in both ammonium- (up-accumulated) and urea-fed (down-accumulated) roots (Fig. 3). Although the presence of RuBisCO in non-photosynthetic tissues is surprising, it has been previously observed in other non-photosynthetic tissues, such as *Arabidopsis* roots (Mooney et al., 2006), oilseed rape embryos and pods (Schwender et al., 2004), and developing seeds and embryos of legumes (Allen et al., 2009; Furbank et al., 2004). In rice (*Oryza sativa*), an unusual RuBisCO small subunit gene (OsRbcS1) was exclusively expressed in non-photosynthetic organs, and highly homologous genes have been found in another species (Morita et al., 2016, 2014). Accordingly, a non-Calvin cycle, CO_2-scanvenging role for RuBisCO has been demonstrated in *Brassica napus* embryos (Schwender et al., 2004). Therefore, the function of the RuBisCO protein in roots under our experimental design may be to accomplish a different function from the RuBisCO found in photosynthetic tissues.

In addition, it is known that phosphoenolpyruvate carboxylases (PEPCs) play a key role during C4 photosynthesis. However, PEPC also participates in a wide range of processes in non-photosynthetic tissues (Izui et al., 2004), as it is considered an anaplerotic enzyme during ammonium-related C-limiting conditions (Ariz et al., 2013). We found a down-accumulation of PEPC1 and PEPC2 in *M. truncatula* roots grown in both N sources. The regulation of non-photosynthetic PEPC, but not of RuBisCO, was maintained in the same way under both urea and ammonium nutrition, which suggest

that the conditions were not greatly stressful and the requirements for C were not high either.

On the other hand, the inhibition of root growth may also be the consequence of the observed up-accumulation of the protein, lipoxygenase (LOX; Medtr8g018420), as previously observed in *A. thaliana* where increase in LOX activity were associated with an altered root phenotype (Vellosillo et al., 2007). In our work, we have observed a significant accumulation of abscisic acid/jasmonate (ABA/JA) signalling-related proteins under ammonium nutrition (Table 1). The activation of the signalling mediated by ABA and JA has been previously associated with abiotic stresses like drought, salt, and ozone as well as interactions between abiotic and biotic stresses (De Vleesschauwer et al., 2014; Nguyen et al., 2016), and so ammonium seems to activate common pathways in the stress response. ABA and JA may also contribute to the stunted root growth by retarding plant growth in response to the stress, as described in earlier work on these hormones (Staswick et al., 1992).

4.2. Membrane proteins are key players in the response of ammonium and urea grown plants

The plasma membrane H^+-ATPase plays a central role in nutrient uptake, intracellular pH maintenance and cell growth, especially in the processes of adaptation to stress conditions (Morsomme and Boutry, 2000). Hence, several studies have described that the H^+-ATPase content is increased under different stresses, suggesting that it might be a central factor for resistance/tolerance. For instance, the involvement of H^+-ATPase activity in salt tolerance has been largely demonstrated by studies of halophytes and salt sensitive plants (Kalampanayil and Wimmers, 2001; López-Pérez et al., 2009; Sahu and Shaw, 2009; Shen et al., 2011). Furthermore, an increased H^+-ATPase activity was proposed as a strategy to prevent an overloading of ammonium in the cell cytoplasm of barley roots grown solely with ammonium (Zhang et al., 2018). In contrast, the up-regulation of plasma membrane H^+-ATPase was not observed in roots of rice grown with ammonium (Zhu et al., 2009). Under our experimental design the down-accumulation of the H^+-ATPase may well be related to the alkalinization of the intracellular pH experienced during ammonium nutrition as the extracellular medium becomes acidified (see Figure 1 Esteban et al., 2016b). This observation is consistent

with the reduction in H^+-ATPase activity caused by the alkalinization of the apoplast in other plant species under different types of stress (Geilfus, 2017).

In addition, Major Intrinsic Proteins (MIPs), which include aquaporins, were found up-accumulated under ammonium and urea nutrition compared to nitrate. The results obtained in our study showed that ammonium and urea nutrition accumulated a MIP, which is annotated as a Plasma membrane Intrinsic Protein (PIP). In general terms, aquaporins are suggested to be involved in water transport in response to N availability, while all types of MIPs have been shown to transport N compounds, including ammonia and urea (M. Wang et al., 2016). Accordingly, it has been shown that different subfamilies of MIPs are able to transport ammonia (NH_3) and urea to some degree, thus maintaining the balance of these two molecules between the cytoplasm and vacuole (Loqué et al., 2005; Wallace and Roberts, 2005; M. Wang et al., 2016). This input of NH_3 as a gaseous and neutral form can induce cytosolic alkalinization due to protonation of ammonia once inside the cell (Ariz et al., 2011; Esteban et al., 2016a). Furthermore, up-accumulation of the aquaporin may underlie the alkalinization of the intracellular pH under ammonium nutrition, as it has been revealed that ammonium nutrition induces a greater input of NH_3 in the neutral form, with its entry possibly being modulated via the different pH levels of cellular compartments. Interestingly, plant species that allow a lower uptake of neutral and gaseous NH_3 show greater tolerance to this type of nutrition (Ariz et al., 2011). Therefore, the differentially expressed MIP may be a candidate to regulate the uptake of NH_3 gas in a beneficial manner for both ammonium and urea grown plants, because in the latter the final product for its assimilation is also ammonium.

4.3. The regulation of the enzymes of phenylpropanoid metabolism contribute to the reinforcement of cell walls under ammonium nutrition

Phenylpropanoid (PP) compounds and their derivatives are common secondary metabolites that control different physiological processes, such as seed dispersal, pigmentation, auxin transport or protection against abiotic stress (Valdés-López and Hernández, 2014). The bulk of the PPs, however, play structural roles in cell walls (Cheynier et al., 2013). For instance, an increase in phenolic compounds and their subsequent incorporation into the cell wall has been described under cold stress, nutrient

deficiencies, UV-radiation, high light or wounding, among others (e.g. Dixon and Paiva, 1995; Griffith and Yaish, 2004).

The role of phenylpropanoid metabolism and the reinforcement of the cell wall has been proposed very recently as a mechanism of adaptation to ammonium nutrition (Vega-Mas et al., 2017; W. Wang et al., 2016). Domínguez-Valdivia et al. (2008) reported that ammonium nutrition induced a different root phenotype in pea plants, which included shorter and probably thicker roots. Esteban et al. (2016b) have also shown shorter roots in *M. truncatula* grown with ammonium as the sole source of N. In the present work, several proteins identified by i-TRAQ were implicated in the modulation of phenylpropanoid biosynthesis, and it is notable that four peroxidase isoenzymes were involved. The phenylalanine ammonia lyase (PAL) protein is the first enzyme affecting both PP, stilbenoid and gingerol biosynthesis. Due to the down-accumulation of PAL and the other two proteins involved in both pathways (caffeoyl-CoA 3-*O*-methyltransferase (CCOMT) and the cytochrome P450 family cinnamate 4-hydroxylase (CyP450 C4H)) we propose that the production of stilbenoid and gingerol from cinnamic acid is repressed. This hypothesis is supported by the finding of greater caffeic acid *O*-methyltransferase (COMT) accumulation, which may act immediately after cinnamic acid degradation, resulting in an increase in the production of PP. Also, the higher POD activity supports this hypothesis because it is involved in the final synthetic step of phenolic compounds such as *p*-hydroxy phenyl lignin, guaiacyl lignin (G) or syringyl lignin (S).

Peroxidases are key players in PP metabolism since they are proposed as the source of radical formation and random coupling to form lignin from monolignols (Boerjan et al., 2003; Hatfield A. W., 2001). It is largely understood that class III peroxidases (CIII-PODs) are mainly located in the cell wall (Welinder, 1992). CIII-PODs consume and generate ROS (Liszkay et al., 2003) and they participate in cell wall dynamics during plant growth (Cosgrove, 2005). Specifically, cell expansion is associated with cell wall loosening and stiffening (Francoz et al., 2015). Under ammonium nutrition, our data showed an up-accumulation of the total POD activities (Fig. 7A). However, no differences in hydrogen peroxide contents among treatments were found (data not shown), suggesting that POD might be implicated in the tolerance response to

ammonium nutrition in *M. truncatula* rather than in the regulation of hydrogen peroxide levels.

Regarding their subcellular localization, the four PODs reported here exhibit the typical long peptide on the C-terminus (Supplementary Figure S3) that in class III peroxidases indicates trafficking through the default secretory pathway (Welinder et al., 2002), but they may well have a role in cell wall formation. Indeed, some of the PODs that have been reported as having a role in lignification also exhibit a longer peptide downstream of the last conserved cysteine (Supplementary Figure S3), such as PRX21 from *Populus trichocarpa*, which has been immunolocalized to the vacuole (Ren et al., 2014).

The capacity to polymerize lignin has been evaluated by the S/G oxidation ratio. Accordingly, those PODs catalysing a higher ratio S/G are considered lignin forming enzymes, while enzymes showing a low S/G ratio are related to peroxidative functions other than lignigication (Shigeto and Tsutsumi, 2016). Furthermore, COMT catalyses the conversion of caffeic acid to ferulic acid (FA) and then to sinapic acid, which is the precursor of syringyl lignin. Thus, the highest accumulation of COMT protein found in ammonium-fed roots, together with the lower FA-dependent POD activity, which is used as G oxidation approach (Fig. 7B), indicates an increase in lignin production under our experimental conditions (Fig. 8). Interestingly, the phylogenetic analysis (Supplementary Figure S4) of the sequences listed in Supplementary Table S3 showed the proximity among three of the *M. truncatula* PODS (POD2, POD6 and POD7) to the BPX1 peroxidase from *Betula pendula*, which after its partial isolation and characterization showed high oxidization rates for lignin precursors (Marjamaa et al., 2006). In Supplementary Figure S5 the high homology present among the 4 *M. truncatula* PODs and BPX1 is shown. In addition, PRX21 is also found within the same phylogenetic clade (clade II) (Supplementary Figure S4). Furthermore, the remaining POD (POD11) is most closely related to OsPrx22, which was shown experimentally to be in the apoplast (Zhou et al., 2011), and to NtPrx60, which is located in the cell wall and also participates in lignin biosynthesis (Blee et al., 2003). As mentioned before, polymerization of the different phenolics may enhance cell wall rigidity and strength, and thereby generate the stunted root growth phenotype observed in the ammonium-fed roots of *M. truncatula* (Fig. 1). In accordance with this suggestion, PODs seem to have

an important role not only in the polymerization of phenolics, but also in stress tolerance.

Thus, the inhibition of root length was associated with an increase in POD in cowpea under salinity (Maia et al., 2013). In cotton and wheat, higher levels of POD activity were found in drought tolerant compared to drought sensitive cultivars (Ranjan et al., 2012; Sečenji et al., 2010). Accordingly, POD-mediated cell-wall stiffening has been proposed as being involved in ammonium- and ABA-inhibited root growth in rice seedlings (Lin and Kao, 2001, 1999). In relation to our findings, an increase in cell wall-bound POD activities followed by an increased lignin content has been suggested as enabling soybean roots to cope with flavonoid-induced stress (Bido et al., 2010). Also, in soybean plants exposed to NaCl, a decrease in root length and PAL activity together with an increase in POD activity has been proposed to strengthen the cell wall and restrict root growth via an enhancement of lignin production (Neves et al., 2010). Moreover, an increase in POD activity was associated with the strengthening of cell walls in leaves of *A. thaliana* grown on ammonium as the only source of N (Podgórska et al., 2017). In the same study, an elevated phenolic content related to cell walls was found, which indicates in addition to the POD increase that cell wall lignification occurred in the leaves in response to ammonium nutrition.

Thus, based on the predicted secretory pathway, the long pro-peptide at the C-terminus, and the phylogenetic relationships to cell-wall-related proteins, as well as our experimental data, it is proposed that the PODs reported here modify root structure in response to ammonium nutrition. Nevertheless, the precise roles of individual PODs in the final steps of lignin biosynthesis in *M. truncatula* will need to be unravelled in future work. In addition, the vascular system is separated from the root cortex by the Casparian strip formed in endodermal cells, which acts as a diffusion barrier (Geldner, 2013). The capacity to regulate the flux of water and nutrients from the cortex to the vascular system in roots also relies on the proper deposition of lignin in the Casparian strip. Thus the lignification of endodermal cells is necessary to establish such a barrier (Naseer et al., 2012). Changes in the lignification of the Casparian strip have been related to loss of the barrier function (Lee et al., 2013), which has been suggested to restrict the uptake of ammonium (Vega-Mas et al., 2017). The induction of lignification has been observed as a response to ammonium in *Arabidopsis* (Podgórska et al., 2017),

salt stress in soybean (Neves et al., 2010) and Cd stress (Rui et al., 2016), among others. Indeed, on the basis of this information from the literature, it seems clear that the identification of up-regulated PODs represents an important underlying mechanism that enables plants to adapt to a high ammonium environment.

5. Conclusions

The present study demonstrates that the mechanism of tolerance to ammonium and urea triggers changes in the expression of 61 proteins. Several groups of proteins are differentially expressed in the C metabolism pathway that are involved in reorganizing N assimilation under ammonium and urea supply. Under ammonium nutrition, the modulation of ammonium uptake, the control of pH and the consumption of energy, which are crucial adaptations during tolerance, involve changes in the expression of 11 membrane proteins. Finally, yet importantly, regulation of the enzymes of phenyl propanoid metabolism leads to an evident enhancement of root cell lignification, which supports the role of the cell wall in tolerance to ammonium nutrition.

Funding: This work was supported by the grants AGL2014-52396-P and AGL2017-86293-P from the Spanish Ministry of Economy and Competitiveness-MINECO. RE received a *Juan de la Cierva-incorporación* grant IJCI-2014-21452. JB is a holder of a PhD fellowship from the Public University of Navarre. The Proteomics Unit of Navarrabiomed is a member of ProteoRed, PRB3-ISCIII-Spain, and is supported by grant PT17/0019/009, of the PE I+D+I 2018-2020 funded by ISCIII and FEDER.

Author Statement

BR conceived and performed experiments, interpreted data and also supervised the whole project and wrote the manuscript. RE contributed to the drafting of the manuscript. JB performed the lignin staining experiment. ES and JF-I supervised the proteomic analyses and contributed to the correction of the manuscript. DB contributed to the writing of the manuscript. JFM conceived and supervised the whole project and the writing of the manuscript.

Acknowledgements: Authors thank all the PRIDE Team for helping to deposit the MS data in ProteomeXChange/PRIDE. Most of the work presented is part of the doctoral thesis of B. Royo, which is deposited at the Public University of Navarra.

References

Allen, D.K., Ohlrogge, J.B., Shachar-Hill, Y., 2009. The role of light in soybean seed filling metabolism. Plant J. 58, 220–234. https://doi.org/10.1111/j.1365-313X.2008.03771.x

Ariz, I., Asensio, A.C., Zamarreño, A.M., García-Mina, J.M., Aparicio-Tejo, P.M., Moran, J.F., 2013. Changes in the C/N balance caused by increasing external ammonium concentrations are driven by carbon and energy availabilities during ammonium nutrition in pea plants: The key roles of asparagine synthetase and anaplerotic enzymes. Physiol. Plant. 148, 522–537. https://doi.org/10.1111/j.1399-3054.2012.01712.x

Ariz, I., Cruz, C., Moran, J.F., González-moro, M.B., García-olaverri, C., González-murua, C., Martins-loução, M.A., Aparicio-tejo, P.M., 2011. Depletion of the heaviest stable N isotope is associated with NH_4^+ / NH_3 toxicity in NH_4^+-fed plants. BMC Plant Biol. 11, 83. https://doi.org/10.1186/1471-2229-11-83

Ariz, I., Esteban, R., García-Plazaola, J.I., Becerril, J.M., Aparicio-Tejo, P.M., Moran, J.F., 2010. High irradiance induces photoprotective mechanisms and a positive effect on NH_4^+ stress in *Pisum sativum* L. J. Plant Physiol. 167, 1038–1045. https://doi.org/10.1016/j.jplph.2010.02.014

Arkoun, M., Sarda, X., Jannin, L., Laîné, P., Etienne, P., Garcia-Mina, J.-M., Yvin, J.-C., Ourry, A., 2012. Hydroponics versus field lysimeter studies of urea, ammonium and nitrate uptake by oilseed rape (*Brassica napus* L.). J. Exp. Bot. 63, 5245–5258.

Bido, G. de S., Ferrarese, M. de L.L., Marchiosi, R., Ferrarese-Filho, O., 2010. Naringenin inhibits the growth and stimulates the lignification of soybean root. Brazilian Arch. Biol. Technol. 53, 533–542. https://doi.org/10.1590/S1516-89132010000300005

Binns, D., Dimmer, E., Huntley, R., Barrell, D., O'Donovan, C., Apweiler, R., 2009. QuickGO: A web-based tool for Gene Ontology searching. Bioinformatics 25, 3045–3046. https://doi.org/10.1093/bioinformatics/btp536

Blee, K.A., Choib, J.W., O'Connella, A.P., Schuchc, W., Lewis, N.G., Bolwell, G.P., 2003. A lignin-specific peroxidase in tobacco whose antisense suppression leads to vascular tissue modification. Phytochemistry 64, 163–176. https://doi.org/10.1016/S0031-9422(03)00212-7

Boerjan, W., Ralph, J., Baucher, M., 2003. Lignin biosynthesis. Annu. Rev. Plant Biol. 54, 519–546. https://doi.org/10.1146/annurev.arplant.54.031902.134938

Britto, D.T., Kronzucker, H.J., 2002. NH_4^+ toxicity in higher plants: a critical review. J. Plant Physiol. 159, 567–584. https://doi.org/10.1078/0176-1617-0774

Cheynier, V., Comte, G., Davies, K.M., Lattanzio, V., Martens, S., 2013. Plant phenolics: Recent advances on their biosynthesis, genetics, andecophysiology. Plant Physiol. Biochem. https://doi.org/10.1016/j.plaphy.2013.05.009

Cordoba-Pedregosa, M., Gonzalez-Reyes, J.A., Canadillas, M., Navas, P., Cordoba, F., 1996. Role of apoplastic and cell-wall peroxidases on the stimulation of root elongation by ascorbate. Plant Physiol. 112, 1119–1125. https://doi.org/10.1104/pp.112.3.1119

Cosgrove, D.J., 2005. Growth of the plant cell wall. Nat. Rev. Mol. Cell Biol. https://doi.org/10.1038/nrm1746

Cox, J., Mann, M., 2008. MaxQuant enables high peptide identification rates, individualized p.p.b.-range mass accuracies and proteome-wide protein quantification. Nat. Biotechnol. 26, 1367–1372. https://doi.org/10.1038/nbt.1511

Cox, J., Neuhauser, N., Michalski, A., Scheltema, R.A., Olsen, J. V., Mann, M., 2011. Andromeda: A peptide search engine integrated into the MaxQuant environment. J. Proteome Res. 10, 1794–1805. https://doi.org/10.1021/pr101065j

Cruz, C., Domínguez-Valdivia, M.D., Aparicio-Tejo, P.M., Lamsfus, C., Bio, A., Martins-Loução, M.A., Moran, J.F., 2011. Intra-specific variation in pea responses to ammonium nutrition leads to different degrees of tolerance. Environ. Exp. Bot. 70, 233–243. https://doi.org/10.1016/j.envexpbot.2010.09.014

De Vleesschauwer, D., Xu, J., HÃ¶fte, M., 2014. Making sense of hormone-mediated defense networking: from rice to *Arabidopsis*. Front. Plant Sci. 5, 1–15. https://doi.org/10.3389/fpls.2014.00611

Dixon, R.A., Paiva, N.L., 1995. Stress-induced phenylpropanoid metabolism. Plant Cell 7, 1085. https://doi.org/10.2307/3870059

Engelsberger, W.R., Schulze, W.X., 2012. Nitrate and ammonium lead to distinct global dynamic phosphorylation patterns when resupplied to nitrogen-starved *Arabidopsis* seedlings. Plant J. 69, 978–995. https://doi.org/10.1111/j.1365-313X.2011.04848.x

Esteban, R., Ariz, I., Cruz, C., Moran, J.F., 2016. Review: Mechanisms of ammonium toxicity and the quest for tolerance. Plant Sci. 248, 92–101. https://doi.org/10.1016/j.plantsci.2016.04.008

Esteban, R., Royo, B., Urarte, E., Zamarreño, Á.M., Garcia-Mina, J.M., Moran, J.F., 2016. Both free indole-3-acetic acid and photosynthetic performance are important players in the response of *Medicago truncatula* to urea and ammonium nutrition under axenic conditions. Front. Plant Sci. 7. https://doi.org/10.3389/fpls.2016.00140

Forde, B.G., 2014. Nitrogen signalling pathways shaping root system architecture: An update. Curr. Opin. Plant Biol. https://doi.org/10.1016/j.pbi.2014.06.004

Francoz, E., Ranocha, P., Nguyen-Kim, H., Jamet, E., Burlat, V., Dunand, C., 2015. Roles of cell wall peroxidases in plant development. Phytochemistry 112, 15–21. https://doi.org/10.1016/j.phytochem.2014.07.020

Furbank, R.T., White, R., Palta, J.A., Turner, N.C., 2004. Internal recycling of respiratory CO_2 in pods of chickpea (*Cicer arietinum* L.): The role of pod wall, seed coat, and embryo. J. Exp. Bot. 55, 1687–1696. https://doi.org/10.1093/jxb/erh190

Geilfus, C.M., 2017. The pH of the apoplast: dynamic factor with functional impact under stress. Mol. Plant 10, 1371–1386. https://doi.org/10.1016/j.molp.2017.09.018

Geldner, N., 2013. The endodermis. Annu. Rev. Plant Biol. 64, 531–558. https://doi.org/10.1146/annurev-arplant-050312-120050

Gerendas, J., Zhu, Z.J., Bendixen, R., Ratcliffe, R.G., Sattelmacher, B., 1997. Physiological and biochemical processes related to ammonium toxicity in higher plants. Zeitschrift fur Pflanzenernahrung und Bodenkd. 160, 239–251. https://doi.org/10.1002/jpln.19971600218

Griffith, M., Yaish, M.W.F., 2004. Antifreeze proteins in overwintering plants: A tale of two activities. Trends Plant Sci. https://doi.org/10.1016/j.tplants.2004.06.007

Grover, A., 2012. Plant chitinases: Genetic diversity and physiological roles. CRC. Crit. Rev. Plant Sci. 31, 57–73. https://doi.org/10.1080/07352689.2011.616043

Hatfield A. W., V.W., 2001. Lignin formation in plants. The dilemma of linkage specificity. Plant Physiol. 126, 34. https://doi.org/10.1104/pp.126.4.1351

Hoepflinger, M.C., Pieslinger, A.M., Tenhaken, R., 2011. Investigations on N-rich protein (NRP) of *Arabidopsis thaliana* under different stress conditions. Plant Physiol. Biochem. 49, 293–302. https://doi.org/10.1016/j.plaphy.2011.01.005

Houdusse, F., Zamarreño, A.M., Garnica, M., García-Mina, J., 2005. The importance of nitrate in ameliorating the effects of ammonium and urea nutrition on plant

development: The relationships with free polyamines and plant proline contents. Funct. Plant Biol. 32, 1057–1067. https://doi.org/10.1071/FP05042

Huerta-Cepas, J., Szklarczyk, D., Forslund, K., Cook, H., Heller, D., Walter, M.C., Rattei, T., Mende, D.R., Sunagawa, S., Kuhn, M., Jensen, L.J., Von Mering, C., Bork, P., 2016. EGGNOG 4.5: A hierarchical orthology framework with improved functional annotations for eukaryotic, prokaryotic and viral sequences. Nucleic Acids Res. 44, D286–D293. https://doi.org/10.1093/nar/gkv1248

Izui, K., Matsumura, H., Furumoto, T., Kai, Y., 2004. Phosphoenol pyruvate carboxylase: A new era of structural biology. Annu. Rev. Plant Biol. 55, 69–84. https://doi.org/10.1146/annurev.arplant.55.031903.141619

Kalampanayil, B.D., Wimmers, L.E., 2001. Identification and characterization of a salt-stress-induced plasma membrane H^+-ATPase in tomato. Plant, Cell Environ. 24, 999–1005. https://doi.org/10.1046/j.1365-3040.2001.00743.x

Lee, Y., Rubio, M.C., Alassimone, J., Geldner, N., 2013. A mechanism for localized lignin deposition in the endodermis. Cell 153, 402–412. https://doi.org/10.1016/j.cell.2013.02.045

Li, B., Li, G., Kronzucker, H.J., Baluška, F., Shi, W., 2014. Ammonium stress in *Arabidopsis*: Signaling, genetic loci, and physiological targets. Trends Plant Sci. 19, 107–114. https://doi.org/10.1016/j.tplants.2013.09.004

Li, G., Li, B., Dong, G., Feng, X., Kronzucker, H.J., Shi, W., 2013. Ammonium-induced shoot ethylene production is associated with the inhibition of lateral root formation in *Arabidopsis*. J. Exp. Bot. 64, 1413–1425.

Li, G., Han, X., Huang, J., Tang, J., 2001. A review of affecting factors of soil nitrogen mineralization in forest ecosystems. Acta Ecologica Sinica, 1187-1195.

Lin, C.C., Kao, C.H., 2001. Abscisic acid induced changes in cell wall peroxidase activity and hydrogen peroxide level in roots of rice seedlings. Plant Sci. 160, 323–329. https://doi.org/https://doi.org/10.1016/S0168-9452(00)00396-4

Lin, C.C., Kao, C.H., 1999. NaCl induced changes in ionically bound peroxidase activity in roots of rice seedlings. Plant Soil 216, 147. https://doi.org/10.1023/A:1004714506156

Liszkay, A., Kenk, B., Schopfer, P., 2003. Evidence for the involvement of cell wall peroxidase in the generation of hydroxyl radicals mediating extension growth. Planta 217, 658–667. https://doi.org/10.1007/s00425-003-1028-1

Liu, Y., Lai, N., Gao, K., Chen, F., Yuan, L., Mi, G., 2013. Ammonium inhibits primary

root growth by reducing the length of meristem and elongation zone and decreasing elemental expansion rate in the root apex in *Arabidopsis thaliana*. PLoS One 8, 1–11. https://doi.org/10.1371/journal.pone.0061031

López-Pérez, L., Martínez-Ballesta, M. del C., Maurel, C., Carvajal, M., 2009. Changes in plasma membrane lipids, aquaporins and proton pump of broccoli roots, as an adaptation mechanism to salinity. Phytochemistry 70, 492–500. https://doi.org/10.1016/j.phytochem.2009.01.014

Loqué, D., Ludewig, U., Yuan, L., von Wirén, N., 2005. Tonoplast intrinsic proteins AtTIP2;1 and AtTIP2;3 facilitate NH_3 transport into the vacuole. Plant Physiol. 137, 671–80. https://doi.org/10.1104/pp.104.051268

Maia, J.M., Voigt, E.L., Ferreira-Silva, S.L., Fontenele, A. V., Macêdo, C.E.C., Silveira, J.A.G., 2013. Differences in cowpea root growth triggered by salinity and dehydration are associated with oxidative modulation involving types I and III peroxidases and apoplastic ascorbate. J. Plant Growth Regul. 32, 376–387. https://doi.org/10.1007/s00344-012-9308-2

Marino, D., Ariz, I., Lasa, B., Santamaria, E., Fernandez-Irigoyen, J., Gonzalez-Murua, C., Aparicio Tejo, P.M., 2016. Quantitative proteomics reveals the importance of nitrogen source to control glucosinolate metabolism in *Arabidopsis thaliana* and *Brassica oleracea*. J. Exp. Bot. 67, 3313–3323. https://doi.org/10.1093/jxb/erw147

Marjamaa, K., Kukkola, E., Lundell, T., Karhunen, P., Saranpää, P., Fagerstedt, K. V., 2006. Monolignol oxidation by xylem peroxidase isoforms of Norway spruce (*Picea abies*) and silver birch (*Betula pendula*). Tree Physiol. 26, 605–611. https://doi.org/10.1093/treephys/26.5.605

McWilliam, H., Li, W., Uludag, M., Squizzato, S., Park, Y.M., Buso, N., Cowley, A.P., Lopez, R., 2013. Analysis tool web services from the EMBL-EBI. Nucleic Acids Res. 41, 597–600. https://doi.org/10.1093/nar/gkt376

Menz, J., Li, Z., Schulze, W.X., Ludewig, U., 2016. Early nitrogen-deprivation responses in *Arabidopsis* roots reveal distinct differences on transcriptome and (phospho-) proteome levels between nitrate and ammonium nutrition. Plant J. 88, 717–734. https://doi.org/10.1111/tpj.13272

Mooney, B.P., Miernyk, J.A., Michael Greenlief, C., Thelen, J.J., 2006. Using quantitative proteomics of *Arabidopsis* roots and leaves to predict metabolic activity. Physiol. Plant. 128, 237–250. https://doi.org/10.1111/j.1399-3054.2006.00746.x

Morita, K., Hatanaka, T., Misoo, S., Fukayama, H., 2016. Identification and expression analysis of non-photosynthetic RuBisco small subunit, OsRbcS1-like genes in plants. Plant Gene 8, 26–31. https://doi.org/10.1016/j.plgene.2016.09.004

Morita, K., Hatanaka, T., Misoo, S., Fukayama, H., 2014. Unusual small subunit that is not expressed in photosynthetic cells alters the catalytic properties of RuBisco in rice. Plant Physiol. 164, 69–79. https://doi.org/10.1104/pp.113.228015

Morsomme, P., Boutry, M., 2000. The plant plasma membrane H^+-ATPase: structure, function and regulation. Biochim. Biophys. Acta - Biomembr. 1465, 1–16. https://doi.org/10.1016/S0005-2736(00)00128-0

Nacry, P., Bouguyon, E., Gojon, A., 2013. Nitrogen acquisition by roots: Physiological and developmental mechanisms ensuring plant adaptation to a fluctuating resource. Plant Soil 370, 1–29. https://doi.org/10.1007/s11104-013-1645-9

Naseer, S., Lee, Y., Lapierre, C., Franke, R., Nawrath, C., Geldner, N., 2012. Casparian strip diffusion barrier in *Arabidopsis* is made of a lignin polymer without suberin. Proc. Natl. Acad. Sci. 109, 10101–10106. https://doi.org/10.1073/pnas.1205726109

Neves, G.Y.S., Marchiosi, R., Ferrarese, M.L.L., Siqueira-Soares, R.C., Ferrarese-Filho, O., 2010. Root growth inhibition and lignification induced by salt stress in soybean. J. Agron. Crop Sci. 196, 467–473. https://doi.org/10.1111/j.1439-037X.2010.00432.x

Nguyen, D., Rieu, I., Mariani, C., van Dam, N.M., 2016. How plants handle multiple stresses: hormonal interactions underlying responses to abiotic stress and insect herbivory. Plant Mol. Biol. 91, 727–740. https://doi.org/10.1007/s11103-016-0481-8

Podgórska, A., Burian, M., Gieczewska, K., Ostaszewska-Bugajska, M., Zebrowski, J., Solecka, D., Szal, B., 2017. Altered cell wall plasticity can restrict plant growth under ammonium nutrition. Front. Plant Sci. 8, 1–19. https://doi.org/10.3389/fpls.2017.01344

Qin, C., Qian, W., Wang, W., Wu, Y., Yu, C., Jiang, X., Wang, D., Wu, P., 2008. GDP-mannose pyrophosphorylase is a genetic determinant of ammonium sensitivity in *Arabidopsis thaliana*. Proc. Natl. Acad. Sci. U. S. A. 105, 18308–18313. https://doi.org/10.1073/pnas.0806168105

Ranjan, A., Pandey, N., Lakhwani, D., Dubey, N.K., Pathre, U. V., Sawant, S. V., 2012. Comparative transcriptomic analysis of roots of contrasting *Gossypium herbaceum*

genotypes revealing adaptation to drought. BMC Genomics 13. https://doi.org/10.1186/1471-2164-13-680

Ren, L.-L., Liu, Y.-J., Liu, H.-J., Qian, T.-T., Qi, L.-W., Wang, X.-R., Zeng, Q.-Y., 2014. Subcellular relocalization and positive selection play key roles in the retention of duplicate genes of *Populus* class III peroxidase family. Plant Cell. https://doi.org/10.1105/tpc.114.124750

Rui, H., Chen, C., Zhang, X., Shen, Z., Zhang, F., 2016. Cd-induced oxidative stress and lignification in the roots of two *Vicia sativa* L. varieties with different Cd tolerances. J. Hazard. Mater. 301, 304–313. https://doi.org/https://doi.org/10.1016/j.jhazmat.2015.08.052

Sahu, B.B., Shaw, B.P., 2009. Salt-inducible isoform of plasma membrane H^+-ATPase gene in rice remains constitutively expressed in natural halophyte, *Suaeda maritima*. J. Plant Physiol. 166, 1077–1089. https://doi.org/10.1016/j.jplph.2008.12.001

Schneider, C.A., Rasband, W.S., Eliceiri, K.W., 2012. NIH Image to ImageJ: 25 years of image analysis. Nat. Methods. https://doi.org/10.1038/nmeth.2089

Schwender, J., Goffman, F., Ohlrogge, J.B., Shachar-Hill, Y., 2004. Rubisco without the Calvin cycle improves the carbon efficiency of developing green seeds. Nature 432, 779–782. https://doi.org/10.1038/nature03145

Sečenji, M., Lendvai, Á., Miskolczi, P., Kocsy, G., Gallé, Á., Szucs, A., Hoffmann, B., Sárvári, É., Schweizer, P., Stein, N., Dudits, D., Györgyey, J., 2010. Differences in root functions during long-term drought adaptation: Comparison of active gene sets of two wheat genotypes. Plant Biol. 12, 871–882. https://doi.org/10.1111/j.1438-8677.2009.00295.x

Shen, P., Wang, R., Jing, W., Zhang, W., 2011. Rice phospholipase Dα is involved in salt tolerance by the mediation of H^+-ATPase activity and transcription. J. Integr. Plant Biol. 53, 289–299. https://doi.org/10.1111/j.1744-7909.2010.01021.x

Shigeto, J., Tsutsumi, Y., 2016. Diverse functions and reactions of class III peroxidases. New Phytol. 209, 1395–1402. https://doi.org/10.1111/nph.13738

Sievers, F., Wilm, A., Dineen, D., Gibson, T.J., Karplus, K., Li, W., Lopez, R., McWilliam, H., Remmert, M., Söding, J., Thompson, J.D., Higgins, D.G., 2011. Fast, scalable generation of high-quality protein multiple sequence alignments using Clustal Omega. Mol. Syst. Biol. 7. https://doi.org/10.1038/msb.2011.75

Stasolla, C., Yeung, E.C., 2007. Cellular ascorbic acid regulates the activity of major

peroxidases in the apical poles of germinating white spruce (*Picea glauca*) somatic embryos. Plant Physiol. Biochem. 45, 188–198. https://doi.org/10.1016/j.plaphy.2007.02.007

Staswick, P.E., Su, W., Howell, S.H., 1992. Methyl jasmonate inhibition of root growth and induction of a leaf protein are decreased in an *Arabidopsis thaliana* mutant. Proc. Natl. Acad. Sci. 89, 6837–6840. https://doi.org/10.1073/pnas.89.15.6837

Unwin, R.D., Griffiths, J.R., Whetton, A.D., 2010. Simultaneous analysis of relative protein expression levels across multiple samples using iTRAQ isobaric tags with 2D nano LC-MS/MS. Nat. Protoc. 5, 1574–1582. https://doi.org/10.1038/nprot.2010.123

Valdés-López, O., Hernández, G., 2014. Phenylpropanoids as master regulators: state of the art and perspectives in common bean (*Phaseolus vulgaris*). Front. Plant Sci. 5, 336. https://doi.org/10.3389/fpls.2014.00336

Vega-Mas, I., Pérez-Delgado, C.M., Marino, D., Fuertes-Mendizábal, T., González-Murua, C., Márquez, A.J., Betti, M., Estavillo, J.M., González-Moro, M.B., 2017. Elevated CO_2 induces root defensive mechanisms in tomato plants when dealing with ammonium toxicity. Plant Cell Physiol. 58, 2112–2125. https://doi.org/10.1093/pcp/pcx146

Vellosillo, T., Martinez, M., Lopez, M.A., Vicente, J., Cascon, T., Dolan, L., Hamberg, M., Castresana, C., 2007. Oxylipins produced by the 9-lipoxygenase pathway in *Arabidopsis* regulate lateral root development and defense responses through a specific signaling cascade. Plant Cell Online 19, 831–846. https://doi.org/10.1105/tpc.106.046052

Vizcaíno, J.A., Csordas, A., del-Toro, N., Dianes, J.A., Griss, J., Lavidas, I., Mayer, G., Perez-Riverol, Y., Reisinger, F., Ternent, T., Xu, Q.-W., Wang, R., Hermjakob, H., 2016. 2016 update of the PRIDE database and its related tools. Nucleic Acids Res. 44, D447–D456.

Wallace, I.S., Roberts, D.M., 2005. Distinct transport selectivity of two structural subclasses of the nodulin-like intrinsic protein family of plant aquaglyceroporin channel. Biochemistry 44, 16826–16834. https://doi.org/10.1021/bi0511888

Wang, M., Ding, L., Gao, L., Li, Y., Shen, Q., Guo, S., 2016. The interactions of aquaporins and mineral nutrients in higher plants. Int. J. Mol. Sci. https://doi.org/10.3390/ijms17081229

Wang, W., Li, R., Zhu, Q., Tang, X., Zhao, Q., 2016. Transcriptomic and physiological

analysis of common duckweed *Lemna minor* responses to NH_4^+ toxicity. BMC Plant Biol. 16, 92. https://doi.org/10.1186/s12870-016-0774-8

Welinder, K.G., 1992. Plant peroxidases: structure - function relationships. Plant Peroxidases 1980-1990, Top. Detail. Lit. Mol. Biochem. Physiol. Asp. 1–24.

Welinder, K.G., Justesen, A.F., Kjærsgård, I.V.H., Jensen, R.B., Rasmussen, S.K., Jespersen, H.M., Duroux, L., 2002. Structural diversity and transcription of class III peroxidases from *Arabidopsis thaliana*. Eur. J. Biochem. 269, 6063–6081. https://doi.org/10.1046/j.1432-1033.2002.03311.x

Zhang, M., Ding, M., Xu, F., Afzal, M.R., Chen, X., Zeng, H., Yan, F., Zhu, Y., 2018. Involvement of plasma membrane H^+-ATPase in the ammonium-nutrition response of barley roots. J. Plant Nutr. Soil Sci. 1–8. https://doi.org/10.1002/jpln.201800045

Zhou, L., Bokhari, S.A., Dong, C.-J., Liu, J.-Y., 2011. Comparative proteomics analysis of the root apoplasts of rice seedlings in response to hydrogen peroxide. PLoS One 6, e16723. https://doi.org/10.1371/journal.pone.0016723

Zhu, Y., Di, T., Xu, G., Chen, X., Zeng, H., Yan, F., Shen, Q., 2009. Adaptation of plasma membrane H^+-ATPase of rice roots to low pH as related to ammonium nutrition. Plant, Cell Environ. 32, 1428–1440. https://doi.org/10.1111/j.1365-3040.2009.02009.x

Zou, N., Li, B., Dong, G., Kronzucker, H.J., Shi, W., 2012. Ammonium-induced loss of root gravitropism is related to auxin distribution and TRH1 function, and is uncoupled from the inhibition of root elongation in *Arabidopsis*. J. Exp. Bot. 63, 3777–3788.

Figure captions

FIGURE 1. Effect of N sources on root length of *M. truncatula* seedlings grown for 15 days under 1 mM nitrate, ammonium or urea in axenic conditions. The bars show the mean ± S.E. (n = 10-15). Different letters denote statistically significant differences at α = 0.05 using the Student–Newman–Keul test.

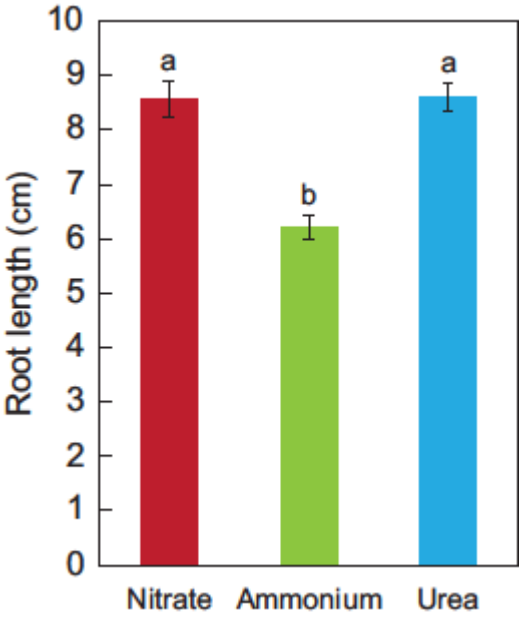

FIGURE 2. Histogram representing the up- and down-accumulation of the 61 differentially identified proteins in *M. truncatula* roots when comparing ammonium *vs*. nitrate, and urea *vs*. nitrate nutrition.

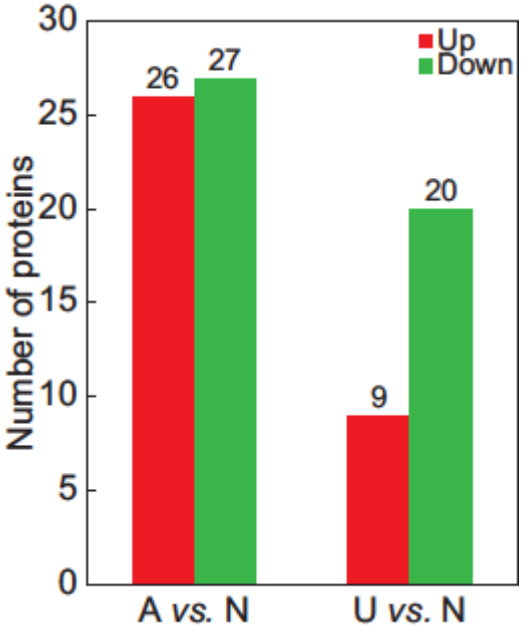

FIGURE 3. Heatmap representing the up- and down-accumulation of the 61 differentially identified proteins in *M. truncatula* roots when comparing ammonium *vs*. nitrate, and urea *vs*. nitrate nutrition.

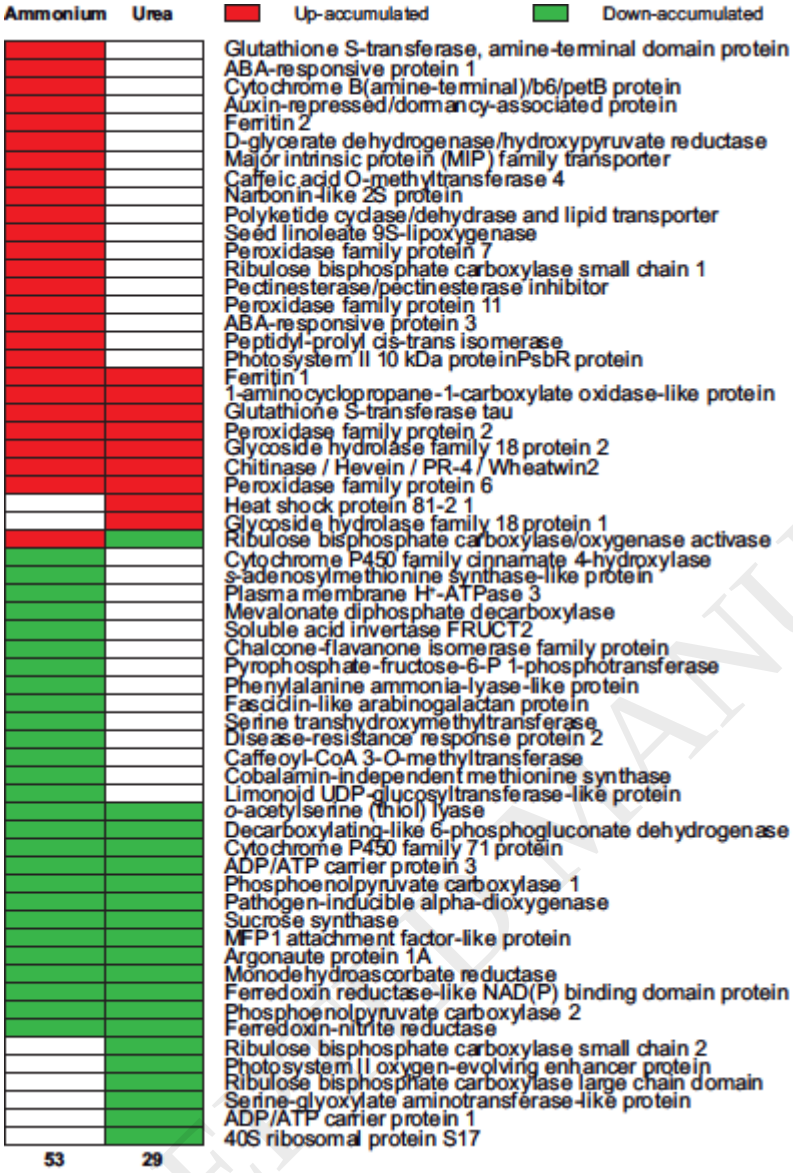

FIGURE 4. Classification of the 61 differentially accumulated proteins according to biological process, cellular component and molecular function on the basis of GO Slim.

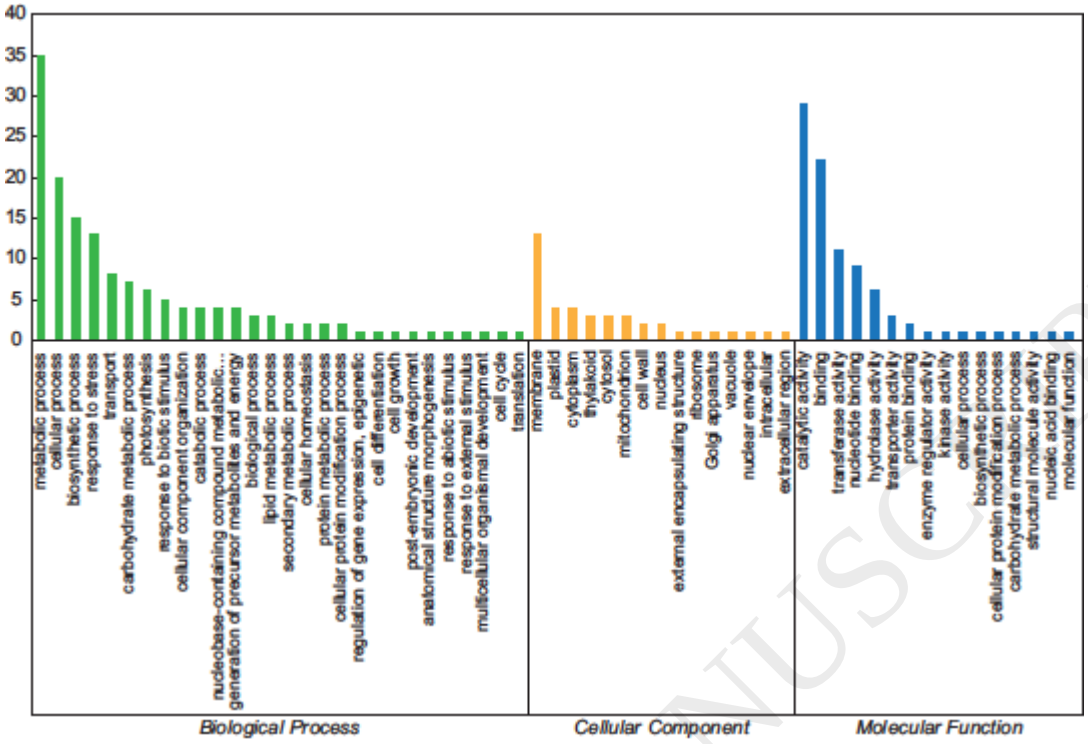

FIGURE 5. Classification of the 61 differentially accumulated proteins into functional categories on the basis of "euKaryiotic Orthologous Groups of proteins" (KOG) when comparing ammonium (**A**) and urea (**B**) nutrition to nitrate treatment.

C: energy production and conversion; D: cell cycle control, cell division, chromosome partitioning; E: amino acid transport and metabolism; G: carbohydrate transport and metabolism; H: coenzyme transport and metabolism. I: lipid transport and metabolism. J: translation, ribosomal structure and biogenesis; M: cell wall/membrane/envelope biogenesis; O: post-translational modification, protein turnover, chaperones; P: inorganic ion transport and metabolism; Q: secondary metabolite biosynthesis, transport and catabolism; S: unknown functions; T: signal transduction mechanisms.

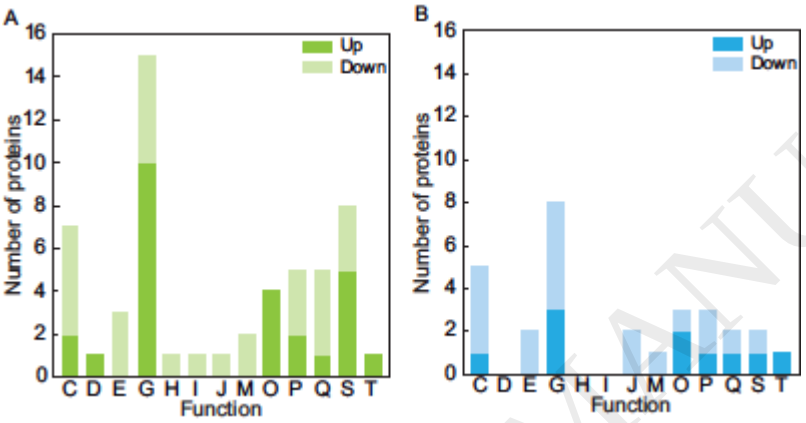

FIGURE 6. The phenylpropanoid biosynthesis pathway of *M. truncatula* roots showing the accumulation followed by the eight affected proteins when comparing ammonium to nitrate nutrition. The up- and down-accumulation of proteins is depicted by respective red and green shading of the name backgrounds.

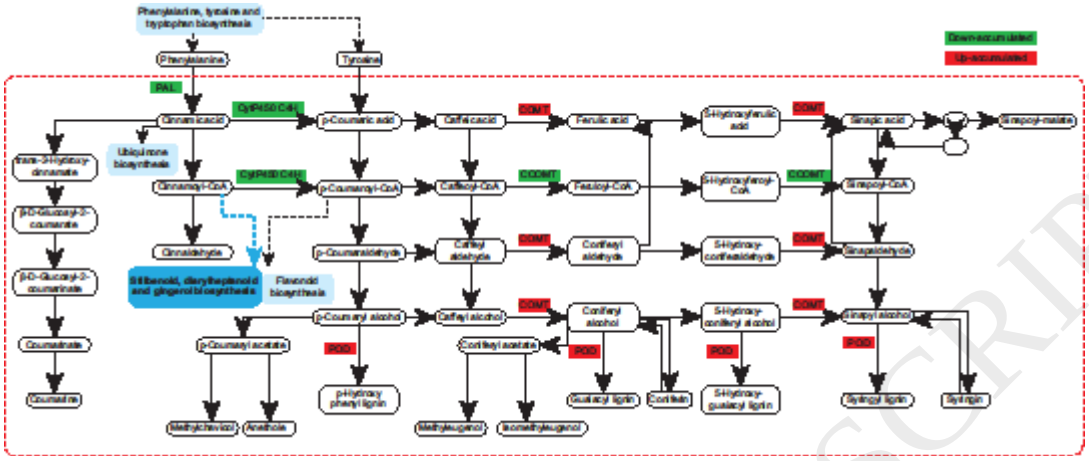

FIGURE 7. Effect of N sources on the guaiacol (**A**) and ferulic acid (**B**) peroxidase activity of *M. truncatula* seedlings grown for 15 days under 1 mM nitrate, ammonium or urea in axenic conditions. The bars show the mean ± S.E. (n = 10-15). Different letters denote statistically significant differences at α = 0.05 using the Student–Newman–Keul test.

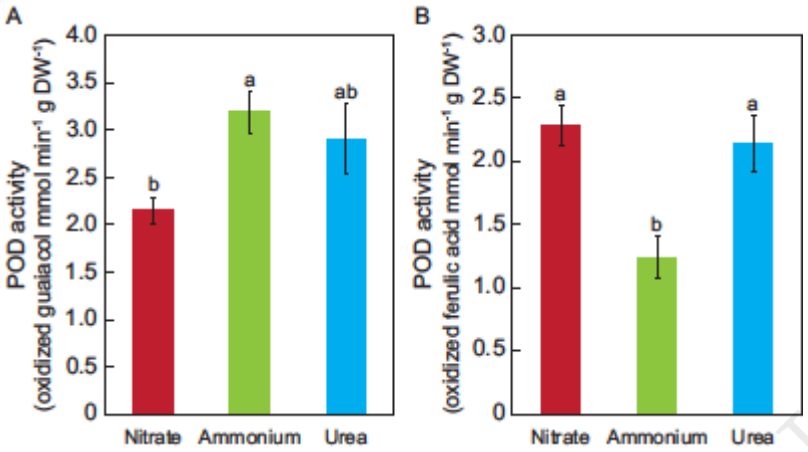

FIGURE 8. Effect of the different N sources on lignin content in *M. truncatula* roots. (**A**) Representative images of lignin staining with Safranin O in *M. truncatula* roots grown on 1 mM nitrate, ammonium, and urea under axenic conditions. (**B**) Quantification of lignin content from the images using ImageJ software. The values are the reciprocal intensity calculated by subtracting the mean ± S.E. (n = 4-5) from 250. Different letters denote statistically significant differences at $\alpha = 0.05$ using the Student-Newman-Keuls test.

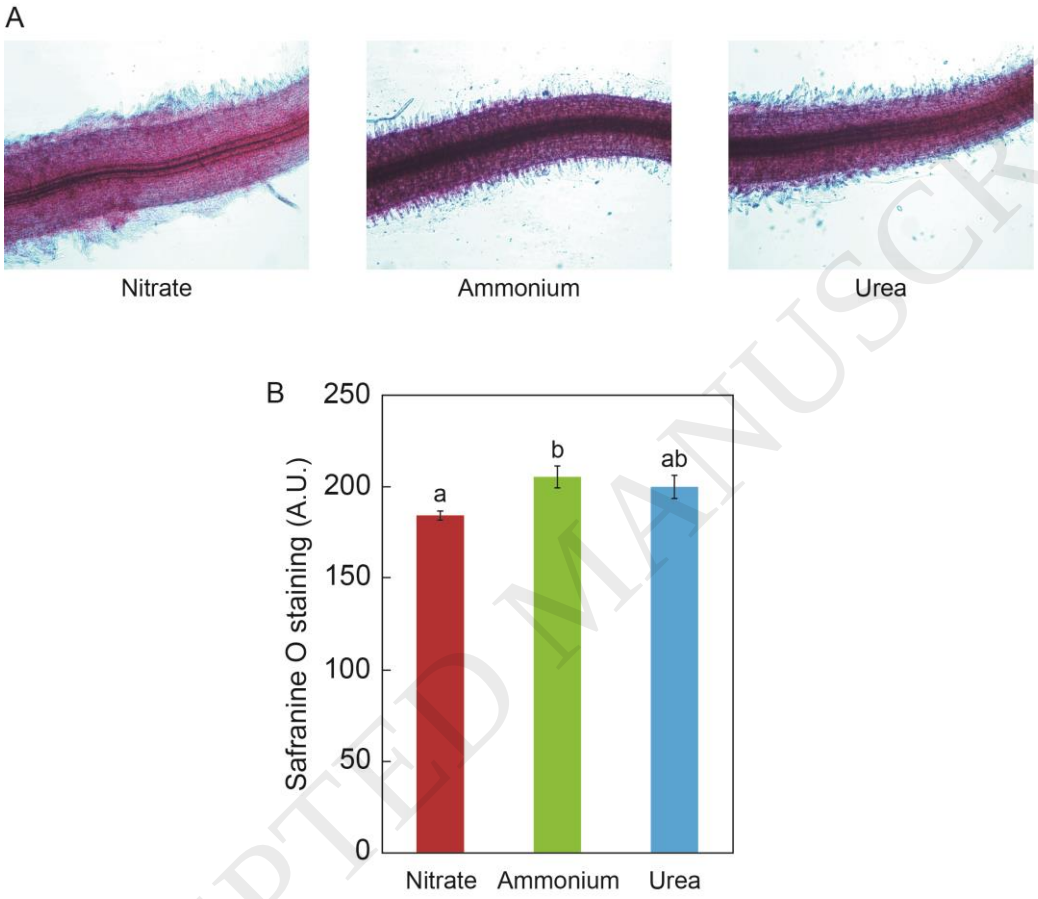

Table 1. List of the 61 differentially identified proteins with a confidence interval (CI) >99% of *M. truncatula* roots grown in axenic culture under nitrate, ammonium, and urea nutrition. The proteins were grouped in accordance with the KOG classification

Uniprot ID	Protein Name	Accession	UP[1]	Score[2]	FC1[3]	FC2[4]	*p*-val[5]
***Energy production and conversion* (C)**							
G7JQB0	Cytochrome B(amine-terminal)/ b6/petB protein	Medtr4g034790	2	16.46	**1.643**	0.843	0.0002
A0A072UGE8	D-glycerate dehydrogenase /hydroxypyruvate reductase	Medtr6g007170	6	54.48	**1.518**	0.982	0.0007
G7LDP4	ADP/ATP carrier protein 1	Medtr8g036880	9	16.98	1.022	**0.695**	0.0044
A0A072UXU6	ADP/ATP carrier protein 3	Medtr4g078545	7	23.30	**0.705**	**0.693**	0.0055
G7IH71	Phosphoenolpyruvate carboxylase 1	Medtr2g076670	25	323.31	**0.682**	**0.752**	0.0014
A0A072VRK6	Limonoid UDP-glucosyltransferase-like protein	Medtr1g107285	3	23.587	**0.627**	1.033	0.0005
G7IKU6	Ferredoxin reductase-like NAD(P) binding domain protein	Medtr2g030200	5	55.54	**0.361**	**0.340**	0.0000
G7IU25	Phosphoenolpyruvate carboxylase 2	Medtr2g092930	11	10.97	**0.331**	**0.574**	0.0011
***Cell cycle control, cell division chromosome partitioning* (D)**							
G7K511	Caffeic acid O-methyltransferase 4	Medtr5g098170	2	12.94	**1.475**	1.053	0.0014
***Amino acid transport and metabolism* (E)**							
G7J014	Serine-glyoxylate aminotransferase-like protein	Medtr3g053890	5	50.33	1.054	**0.682**	0.0019
G7JNN9	O-acetylserine (thiol) lyase	Medtr4g087520	6	78.63	**0.753**	**0.687**	0.0039
G7LH57	Serine transhydroxymethyltransferase	Medtr8g081510	9	18.62	**0.680**	1.035	0.0010
G7L0I7	Cobalamin-independent methionine synthase	Medtr7g086300	37	323.31	**0.635**	1.141	0.0034

***Carbohydrate transport and metabolism* (G)**							
A4UN77	Peroxidase family protein 2	Medtr2g029750	9	323.31	**1.674**	**1.448**	0.0079
A0A072TLJ8	Glycoside hydrolase family 18 protein 2	Medtr0002s1060	15	179.97	**1.532**	**1.315**	0.0002
Q946J9	Major intrinsic protein transporter	Medtr5g082070	5	15.58	**1.485**	1.241	0.0026
G7IG38	Narbonin-like 2S protein	Medtr0062s0090	4	26.03	**1.453**	0.997	0.0075
G7IJU5	Peroxidase family protein 6	Medtr2g029850	5	169.31	**1.419**	**1.340**	0.0084
G7IJV0	Peroxidase family protein 7	Medtr2g029910	2	43.96	**1.411**	1.135	0.0080
B7FHB2	Ribulose bisphosphate carboxylase small chain 1	Medtr6g018310	10	185.68	**1.403**	0.852	0.0003
Q2HRX3	Pectinesterase/pectinesterase inhibitor	Medtr7g050980	9	89.38	**1.393**	1.231	0.0019
A0A072UAE2	Peroxidase family protein 11	Medtr6g043240	10	256.16	**1.391**	0.955	0.0020
G7IJ45	Photosystem II 10 kDa proteinPsbR protein	Medtr2g064650	3	17.38	**1.344**	0.867	0.0018
A0A072TXF3	Ribulose bisphosphate carboxylase small chain 2	Medtr7g007220	8	64.95	1.298	**0.728**	0.0008
G7ZVI4	Photosystem II oxygen-evolving enhancer protein	Medtr8g078870	10	154.31	1.213	**0.722**	0.0011
G7JG19	Ribulose bisphosphate carboxylase large chain domain protein	Medtr4g051270	23	323.31	1.063	**0.595**	0.0001
G7ZXA1	Glycoside hydrolase family 18 protein 1	Medtr0062s0170	10	174.32	0.810	**1.407**	0.0002
A0A072TUR1	Decarboxylating-like 6-phosphogluconate dehydrogenase	Medtr8g099185	11	80.481	**0.736**	**0.768**	0.0008
A0A072V0J5	Soluble acid invertase FRUCT2	Medtr4g101630	6	64.33	**0.731**	1.004	0.0072
A0A072V1H8	Chalcone-flavanone isomerase family protein	Medtr3g093980	3	26.17	**0.713**	0.870	0.0027
Q2HTG9	Pyrophosphate-fructose-6-phosphate 1-phosphotransferase	Medtr2g025020	5	36.30	**0.695**	0.884	0.0042

A0A072VRK6	Limonoid UDP-glucosyltransferase-like protein	Medtr1g107285	3	23.587	**0.627**	1.033	0.0005
***Coenzyme transport and metabolism* (H)**							
A4PU48	*S*-adenosylmethionine synthase-like protein	Medtr7g110310	14	131.47	**0.759**	1.052	0.0009
***Lipid transport and metabolism* (I)**							
A0A072W240	Mevalonate diphosphate decarboxylase	Medtr1g112230	4	42.34	**0.732**	0.984	0.0059
***Translation, ribosomal and biogenesis* (J)**							
I3SPL5	40S ribosomal protein S17	Medtr1g058250	3	25.39	0.821	**0.735**	0.0050
A0A072UAR8	Argonaute protein 1A	Medtr6g477980	2	43.28	**0.602**	**0.592**	0.0005
***Cell wall/membrane/envelope biogenesis* (M)**							
G7K0M1	Fasciclin-like arabinogalactan protein	Medtr5g098420	2	13.56	**0.684**	1.124	0.0003
Q9T0M6	Sucrose synthase	Medtr4g124660	28	323.31	**0.638**	**0.578**	0.0003
***Post-translational modification, protein turnover and chaperones* (O)**							
G7JPE9	Glutathione S-transferase, amine-terminal domain protein	Medtr4g059730	4	41.67	**1.801**	0.954	0.0002
A0A072VLL6	Glutathione S-transferase tau	Medtr1g067180	5	50.89	**1.713**	**1.365**	0.0005
A0A072VNE4	Peptidyl-prolyl cis-trans isomerase	Medtr1g085560	4	33.04	**1.351**	1.114	0.0068
A0A072UYT5	RuBisCO activase	Medtr3g068030	24	323.31	**1.301**	**0.726**	0.0035
G7K4R2	Heat shock protein 81-2 1	Medtr5g096460	45	323.31	1.000	**1.321**	0.0033
***Inorganic ion transport and metabolism* (P)**							
G7JLS7	Ferritin 1	Medtr4g014540	6	50.15	**2.732**	**1.544**	0.0000

G7K283	Ferritin 2	Medtr5g083170	5	29.15	**1.527**	1.092	0.0010
G7JUD2	Plasma membrane H+-ATPase 3	Medtr4g127710	23	293.12	**0.734**	0.931	0.0043
A0A072U5J4	Monodehydroascorbate reductase	Medtr8g098910	8	94.56	**0.560**	**0.580**	0.0000
G7JL79	Ferredoxin-nitrite reductase	Medtr4g086020	5	32.44	**0.312**	**0.326**	0.0000
***Secondary metabolites biosynthesis, transport and catabolism* (Q)**							
A0A072VEZ8	1-aminocyclopropane-1-carboxylate oxidase-like protein	Medtr1g032220	2	11.58	**1.824**	**1.353**	0.0001
Q2MJ09	Cytochrome P450 family cinnamate 4-hydroxylase	Medtr5g075450	3	18.81	**0.765**	0.828	0.0028
G7KEE9	Cytochrome P450 family 71 protein	Medtr5g072980	4	44.29	**0.724**	**0.621**	0.0031
A0A072U4G3	Phenylalanine ammonia-lyase-like protein	Medtr7g101395	2	12.48	**0.690**	0.822	0.0015
G7JK14	Caffeoyl-CoA 3-O-methyltransferase	Medtr4g085590	5	40,31	**0.663**	1.130	0.0033
***Function unknown* (S)**							
G7IMZ3	ABA-responsive protein 1	Medtr2g035190	11	30.55	**1.785**	0.991	0.0007
A0A072V3F7	Auxin-repressed/dormancy-associated protein	Medtr2g014240	4	78.68	**1.566**	1.251	0.0088
I3T9Y8	Polyketide cyclase/dehydrase and lipid transporter	Medtr1g030820	14	206.99	**1.447**	1.243	0.0016
G7LI99	Seed linoleate 9S-lipoxygenase	Medtr8g018420	26	323.31	**1.420**	1.154	0.0072
G7INA7	ABA-responsive protein 3	Medtr2g035220	11	38.92	**1.384**	1.084	0.0021
G7IMY7	Disease-resistance response protein 2	Medtr2g035120	9	103.35	**0.664**	0.892	0.0009
A0A072U6C1	Pathogen-inducible alpha-dioxygenase	Medtr6g007763	5	7.18	**0.648**	**0.714**	0.0013
A0A072V335	MFP1 attachment factor-like protein	Medtr3g102500	2	28.59	**0.625**	**0.692**	0.0043
***Signal transduction mechanisms* (T)**							

A0A072U5A4	Chitinase / Hevein / PR-4 / Wheatwin2	Medtr7g115220	2	40.86	1.436	1.353	0.0064

[1] Number of peptides that are unique in the cited protein.[2] Quality of the identification of the protein represented as the sum of the individual SCORE of each peptide that conforms to the protein. [3] Difference in the intensity of the protein expressed as the fold change (FCs) when comparing NH_4^+ *vs*. nitrate nutrition. [4] Difference in the intensity of the protein expressed as the fold change when comparing urea *vs*. nitrate nutrition. FCs are depicted in red for up-regulated proteins and in green for down-regulated proteins. [5] *p*-value of the ANOVA test

Table 2. Differentially identified proteins implied in the phenylpropanoid biosynthesis pathway. The protein name, the accession and the identification from UniProt is provided. UniProt ID is depicted in red for up-accumulated proteins and in green for down-accumulated proteins.

Protein Name	Accession	UniProt ID
Caffeic acid O-methyltransferase (COMT)	gi|657386071|	G7K511
Caffeoyl-CoA 3-O-methyltransferase (CCOMT)	gi|355508982|	G7JK14
Cytochrome P450 family cinnamate 4-hydroxylase (CyP450 C4H)	gi|355517372|	Q2MJ09
Peroxidase family protein 11	gi|657382113|	A0A072UAE2
Peroxidase family protein 2	gi|355483535|	A4UN77
Peroxidase family protein 6	gi|355483545|	G7IJU5
Peroxidase family protein 7	gi|355483550|	G7IJV0
Phenylalanine ammonia-lyase-like protein (PAL)	gi|657379705|	A0A072U4G3